INSTITUTE OF PHYSICS PUBLISHING SMART MATERIALS AND STRUCTURES
Smart Mater. Struct. **14** (2005) 1010–1016 doi:10.1088/0964-1726/14/5/039

Investigations on an electronic tongue with polymer microfluidic cell for liquid sensing and identification

Stefany Jacesko[1], Jose K Abraham[1], Taeksoo Ji[1], Vijay K Varadan[1], Marina Cole[2] and Julian W Gardner[2]

[1] Department of Electrical Engineering, University of Arkansas, Fayetteville, AR 72701, USA
[2] School of Engineering, University of Warwick, Coventry, UK

Received 12 May 2005, in final form 28 June 2005
Published 2 September 2005
Online at stacks.iop.org/SMS/14/1010

Abstract
Design and experimental results of a surface acoustic wave (SAW) microsensor with polymer microfluidic cell for the sensing and identification of liquids is presented in this paper. This microsensor, which is a part of a smart tongue–nose system, uses a horizontally polarized SAW (SH-SAW) for the detection and identification of liquids. The SH-SAW microsensors are fabricated on 36°-rotated Y-cut X-propagating $LiTaO_3$ ($36YX$.LT) substrate. This design consists of a dual-delay-line configuration in which one line is free and other one is metallized and shielded. Polymer microfluidic cells were designed and fabricated on top of it using a microstereolithography system to avoid dielectric loading of the IDTs by liquid which leads to unwanted dielectric sensitivity to the sensor. Due to the high electromechanical coupling of the $36YX$.LT substrate, it could detect differences in electrical properties and hence distinguish different liquids. It is clear from these results that the microsensor based on $36YX$.LT is an effective liquid identification system for the electronic tongue application.

(Some figures in this article are in colour only in the electronic version)

1. Introduction

Until recently, the distinction of one liquid from another has depended mainly on human sensory tests, where the results are based on subjective judgment. With the development of a reliable liquid sensor with real time readouts, the classification of a liquid substance will be available within a specified repeated accuracy. These sensors are important for use in commercial applications such as testing the freshness of milk and acidity levels of fruit juices. They are important when concerned with heath and safety issues such as blood and urine analysis and they are targeted for use in homeland security for the detection of chemical and biological hazards.

Surface acoustic wave (SAW) microsensors are a unique class of devices that have been used as electronic tongues and noses because the propagating acoustic waves can effectively couple with the medium placed in contact with the device surface. The interaction between acoustic waves and mass density, elastic stiffness and electric/dielectric properties of the propagating medium can give the sensing response. Any changes in the above properties can be measured as changes in phase or amplitude of the propagating waves. Detection of electro-acoustic properties of many liquids using the acoustic microsensors is reported in [1–3]. Many attempts were made using surface waves for detection of liquid level [4], leaky SAW modes for biosensors and viscosity sensors [5, 6], multimode SAW delay lines to measure acoustic properties of liquids [7], liquid sensors using dual-mode delay lines [8], estimation of components [9] and identification of liquids [10–13]. The response can be related to physical quantities such as mass density and viscosity.

These microsensors offers a number of advantages over traditional sensors, including real-time electronic readout, small size, robustness and a low cost of fabrication. One of the issues of this sensor is the change in impedance of the IDTs due to the presence of any liquid over it, and it gives unwanted

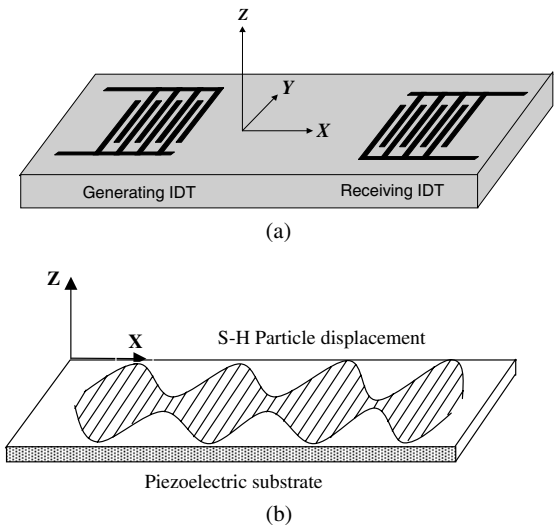

Figure 1. (a) Schematic diagram of the surface acoustic wave (SAW) sensor; (b) shear-horizontal displacement of the particles.

sensitivity with respect to the electrical properties of liquid. To avoid spreading of any liquid over the IDTs, a polymer microfluidic cell is designed and fabricated on top of a dual-line acoustic microsensor on $LiTaO_3$ substrate as a part of a smart tongue–nose system for the identification of liquids. The liquid under test is directed only over the wave propagation path and the IDTs are protected from the influence of the liquids. The measurement results reported in this paper establish that identification is easily possible using this microsensor.

2. Theory

In a Raleigh-SAW device, the wave propagates with most of its energy confined to one acoustic wavelength on the surface. The wave involves a retrograde elliptical motion of particles on the substrate with both in-plane and out-of-plane motions and is generated and detected using inter-digital transducers (IDTs) as shown in figure 1. Physical motion of the particles at the substrate surface along the Z axis is larger than the displacement along the X direction as shown in figure 1(b). The amplitude of both these displacements becomes negligible for penetration depth greater than one wavelength [14]. In liquid based applications, the out-of-plane motion can induce large losses due to the propagation of acoustic waves into the liquid. To avoid the loss, a shear horizontal polarized mode (SH-SAW) can be used to realize a liquid–phase sensor so that the propagation along the solid–liquid interface can occur without the out-of-plane component. It is known that the SAW wave traveling on a 36° rotated Y-cut X-propagating $LiTaO_3$ substrate is a pseudo-type shear horizontal mode and the damping of waves due to liquid in such microsensors is negligible [15].

The SH-SAW wave that propagates on the surface of $36YX$.LT has an electric field that extends several micrometers into the liquid. The acousto-electric interaction with the liquid affects the velocity and/or attenuation of SH-SAW wave propagation and this principle is used for sensing the dielectric properties of the liquids being tested. Characterization of such devices in terms of sensitivity, temperature dependence and mass loading is established in [16].

In the absence of a liquid, acoustic conductance $G(\omega)$ is related to the conductance at center frequency G_0, as well as the angular frequency ω of the device, and can be written as [3]

$$G(\omega) = G_0\left[\frac{\sin(\omega)}{\omega}\right]^2 \tag{1}$$

$$\omega = \pi N\frac{\omega - \omega_0}{\omega_0}. \tag{2}$$

The angular frequency is a function of the number of finger pairs N, and the center frequency ω_0. The conductance at the center frequency G_0 is a function of the geometry of the device, as well as the resistance, given by

$$G_0 = 2.25\omega_0 N^2 W(\varepsilon_0 + \varepsilon_S)\frac{K^2}{2} \tag{3}$$

where W is the aperture of the electrodes and ε_0 and ε_S are the permittivity of air and of the piezoelectric substrate, respectively. The electromechanical coupling coefficient of the substrate K is dependent on the crystal cut, center frequency of the device and the mechanical properties and thickness of the IDT metallization.

The acoustic susceptance $B(\omega)$ is related to reactance, mass and stiffness susceptance. Mass susceptance is inversely proportional to frequency. Resonance occurs when mass and stiffness are proportional in magnitude.

$$B(\omega) = G_0\left[\frac{\sin(2\omega) - 2\omega}{2\omega^2}\right]. \tag{4}$$

The current I is determined by the static capacitance C of the electrodes and the acoustic admittance. The acoustic admittance is the acoustic conductance when added to the acoustic susceptance $[G(\omega) + B(\omega)]$. The acoustic admittance represents the ease with which acoustic energy passes through the system. The input admittance of the transmitter IDT is given by [16]

$$A_{11}(\omega) = \frac{I_1}{V} = G(\omega) - \mathrm{j}B(\omega) + \mathrm{j}\omega C. \tag{5}$$

Due to reciprocity, the input admittance of the receiver IDT A_{22} is equal to the input admittance of the transmitter IDT A_{11}. Therefore, the complex unperturbed admittance transfer function for transmitter to receiver can be approximated as

$$A_{12}(\omega) = G(\omega)\alpha\exp(-\mathrm{j}2\pi L/\lambda) \tag{6}$$

$$\tau_{SH} = \frac{L}{v} = \frac{L}{f\lambda} \tag{7}$$

where the delay time τ_{SH} has been substituted with $L/f\lambda$. L is the distance between the centers of the transducers, λ is the wavelength, α is the attenuation coefficient and v is the phase velocity.

With the addition of a liquid in the liquid sensing region, there are changes that have to be made to the admittance transfer function. We now have to account for changes in the delay time and attenuation of the wave. These factors must

be added to the admittance transfer function as an additional phase shift and attenuation. The equation for the admittance transfer function in the perturbed case is then represented as

$$A_{12}(\omega) = G(\omega)\alpha \exp\left(-\frac{\mathrm{j}2\pi L}{\lambda}\right) \exp\left(\frac{\mathrm{j}2\pi \delta l}{\lambda}\right) \exp(\alpha l) \quad (8)$$

where $\delta = \Delta v/v$ is the fractional velocity change of the device due to the sensing effect, l is the length of the liquid contact area, and α is the attenuation of the SH-SAW due to the sensor effect along l. Since the change in electrical parameters leads to the perturbation in phase velocity and attenuation, the fractional velocity and attenuation change can be written as [17, 18]

$$\frac{\Delta v}{v} = -\frac{K_s^2}{2} \frac{(\sigma'/\omega)^2 + \varepsilon_0(\varepsilon_r' - \varepsilon_r)(\varepsilon_r'\varepsilon_0 + \varepsilon_P^T)}{(\sigma'/\omega)^2 + (\varepsilon_r'\varepsilon_0 + \varepsilon_P^T)^2} \quad (9)$$

$$\frac{\Delta \alpha}{k} = \frac{K_s^2}{2} \frac{(\sigma'/\omega)(\varepsilon_r\varepsilon_0 + \varepsilon_P^T)}{(\sigma'/\omega)^2 + (\varepsilon_r'\varepsilon_0 + \varepsilon_P^T)^2} \quad (10)$$

where ε_P^T is the effective permittivity of the crystal, ε_r is the permittivity of the reference liquid, ε_r' and σ' are the permittivity and conductivity related to loss of the measurand, and k is the wavenumber. The changes in velocity and attenuation of the SH-SAW in the two delay lines are functions of permittivity, conductivity, viscosity and density of the liquid. However, since the free line as well as the shorted lines are on the same substrate, the temperature effect is common for both lines. Since we consider the liquid under test is an isotropic thin film of thickness h and density σ, uniformly loading the metallized surface [16],

$$\left(\frac{\Delta v}{v}\right)_{\text{free}} = f(\varepsilon, \sigma, \eta, \rho, T) \quad (11)$$

$$\left(\frac{\Delta v}{v}\right)_{\text{shorted}} = f(\eta, \rho, T) \quad (12)$$

$$\frac{\Delta \alpha}{k} = 0. \quad (13)$$

2.1. pH and electrical conductivity

The electrical conductivity (EC) of a solution is a measure of its ability to conduct electricity. The EC (μS cm^{-1}) increases with the increase in the presence of ions (salts). EC also depends on the total number of dissolved ions in the water, which is highly dependent on the temperature. pH is a measure of the acidity or alkalinity of solution, expressed in terms of concentration of hydrogen ions or pH $= -\log[\mathrm{H}^+]$. The total conductivity, which has an empirical linear relationship with ionic concentration, depends on the concentration of the ionic species and its conductance, and can be written as [19]

$$\lambda_k = \sum^{n} [|z|M^z]_j \lambda_{ij},$$

where λ_{ij} is the equivalent ionic conductance of the jth species in the solution and M_j is the concentration of the ionic species.

2.2. Principal component analysis

Principal component analysis (PCA) is a mathematical procedure that reduces the number of variables in the analysis; at the same time it can detect a relationship of variables that are not measured in the same units. An example would be trying to monotonically relate the underlying factors in environmental effects such as temperature, pH, density, and phase shift. Essentially, PCA takes a cloud of data points and rotates it such that the maximum variability is visible. In technical terms, PCA identifies the most important gradients in the given data.

$$S_P^2 = \frac{(n_1 - 1)S_1^2 + (n_2 - 1)S_2^2}{(n_1 + n_2 - 2)}. \quad (14)$$

The first step in rotating the data cloud is to standardize the data by subtracting the mean and dividing by the standard deviation. Thus, the centroid of the whole data set is zero. Three standardized axes (1, 2, 3) become comparable to the Cartesian coordinate system, in that axis 1 is orthogonal to axis 2, and axis 3 is orthogonal to 1 and 2. PCA chooses the first axis as the line that goes through the centroid, but also minimizes the square of the distance of each point to the line. Equivalently, the line goes through the maximum variation in the data. The second PCA axis also must go through the centroid, and also through the maximum variation in the data, but as stated previously must be orthogonal to axis 1. Therefore, PCA is either an eigenanalysis of the covariance matrix or an eigenanalysis of the correlation matrix, depending on whether or not the data are standardized. Statistical packages, such as Uni-Stat[3], MATLAB[4], or Minitab[5], were used for data analysis.

It is possible to reduce the parameters in the electronic tongue analysis to two by taking the ratios and/or differences of the free and shorted delay lines for phase and attenuation shift. Pre-processing parameters are often used to better the output of the PCA analysis. These pre-processing parameters include the phase difference between the shorted and free delay lines, the phase ratio, amplitude difference, and amplitude ratio of the shorted and free delay lines.

The analysis can be done by the Fisher t-test or any other rudimentary statistical analysis testing applicable. From this test we can make inferences about the entire population of results from our measured sample group. The equation used in this statistical Fisher t-test is given, by which the pooled estimate of the standard deviation S_p can be determined from

$$t = \frac{(\bar{x}_1 - \bar{x}_2)}{S_p\sqrt{\frac{1}{n_1} + \frac{1}{n_2}}}. \quad (15)$$

3. Device fabrication and testing

The SH-SAW device is fabricated on a 36YX.LT substrate with Au/Cr metallization. As shown in figure 2, this device is a dual-delay-line configuration with a microfluidic cell on top of it. One delay path is electrically shorted by an Au/Cr film and the other path has an opening to the substrate. The electrically

[3] www.unistat.com
[4] www.mathworks.com
[5] www.minitab.com

Table 1. Design parameters of the SAW microsensor.

Parameter		Value
Frequency of operation		55–65 MHz
Finger spacing		34 μm
IDT finger width		17 μm
Acoustic spacing		7513 μm
Number of fingers		28
SH-SAW velocity (m s^{-1})		
Air/36YX.LT	Free surface	4212.6
	Metallized	4114.1
Water/36YX.LT	Free surface	4161.5
	Metallized	4110.8

shorted side is used as the reference and the open side is used for sensing. The operating parameters of the SAW devices are given in table 1. A polymeric microfluidic cell is fabricated on top of the device using the microstereolithography system as explained in section 4. When the liquid is injected into the liquid cell, the liquid and the electric potential acousto-electrically interact over the electrical opening area and the SH-SAW is agitated. The SH-SAW is also perturbed by the viscosity and mass-loading of the liquid, but these mechanical perturbations arise on both the surfaces and can be eliminated due to the dual-delay configuration.

Several requirements have been taken into consideration in the design of the SH-SAW liquid sensors. The size of the device, the number of transducer fingers and the bandwidth of the sensor output have to be determined. The sensitivity and rise time due to the thermal properties are improved with small devices. The bandwidth of the sensor output is mainly dependent on the number of transducer fingers. Increasing the number of fingers increases the acoustic loading while decreasing the bandwidth. On the other hand, in order to minimize the device capacitance the number of fingers should be kept low. However, to minimize the conversion losses, the number of fingers should be large and diffraction losses can be kept low by using a large aperture. By considering all the above factors, the SH-SAW sensors can be designed in a dual-delay-line configuration with a 10 mm $\times$ 7.5 mm die. Parameters derived and used for the design and fabrication of the microsensor on $LiTaO_3$ substrate are shown in table 1.

4. Fabrication of microfluidic cell

The principle used for sensing the dielectric properties of the liquids is the acousto-electric interaction of the liquid with acoustic waves, that affects the velocity and/or attenuation of SH-SAW waves. However, the input impedance of the microsensor IDTs will change due to the presence of any liquid over them. The dielectric loading of the IDTs by the liquid also leads to unwanted sensitivity with respect to the electrical properties of the liquid. To overcome these issues, a microfluidic cell is designed and fabricated on top of the microsensor using a microstereolithography (MSL) system so that the liquid is being directed only over the wave propagation path [20, 21]. As shown in figure 3, three-dimensional MSL is based on the photo-polymerization of liquid monomers using ultraviolet (UV) radiation [22, 23]. The microfluidic cell is used to isolate the liquid from the acousto-electric transducers of the delay lines. MSL is a simple, precise and space efficient technique with the smallest amount of bulk material possible. The microfluidic cell is fabricated using 1.6 hexanediol diacrylate (HDDA) monomer and the objects are built layer by layer on the substrate. The design layout of the object to be built is sent to the XY–Z moving stage controller and the computer. The CAD image is focused and projected on the surface of a photopolymerizable resin. A selective polymerization of the liquid resin occurs in the irradiated areas. A pattern generator is used to shape the UV light beam into the selected pattern. The shutter occults the UV light when a layer is solidified. The object is then lowered into the photoreactor and a new layer of resin is spread on the surface of the already polymerized part. When the liquid surface has been stabilized, the irradiation of the next layer will start.

Table 2. Dimensions of the microfluidic cell fabricated using MSL.

Post length	4 mm
Post height	5 mm
Channel height	3 mm
Roof height	0.3 mm
Top gap	4 mm
Post width	3 mm
Side gap	9 mm
Side wall	17 mm

The dimensions of the microfluidic cell are shown in table 2. The volume of the cell is 10 ml. The translucent liquid cell is positioned accurately over the sensing area between the IDTs, leaving the channel walls to rest on the actual device. The liquid cell prevents the spreading of the liquid into the IDT areas which may cause change in input impedance and electrical load influence. Care is also taken while doing the actual testing in administering the liquid, removing the liquid and cleaning the cell.

The amplitude and phase of the device are measured using an HP8714ET RF network analyzer. A frequency sweep is maintained for viewing both the attenuation and phase. IPA and de-ionized (DI) water are used to clean the devices between tests. IPA is flushed over the device between tests and then the device is continuously flushed with DI water until the original values in amplitude and phase are reached.

Different liquids and soft drinks such as Strawberry Hi-C, Fruit Punch Hi-C, Margarita Mixer, Bloody Mary Mixer, and teriyaki sauce were tested using the device. The pH levels in DI water were also varied and tested by the addition of either hydrochloric acid or sodium hydroxide (base).

The network analyzer was calibrated from 55 to 65 MHz. The center frequency was found to be approximately 59.603 MHz on the free side and 59.773 MHz on the shorted side. The associated insertion loss for the free side was found to be about -9.652 and -7.673 dB on the shorted side. The initial phase was 107.65° on the free side, and -46.763° on the shorted side.

5. Results and discussions

Figure 4 shows the measured results for Strawberry Hi-C, Fruit Punch Hi-C, Margarita Mixer, Bloody Mary Mixer, teriyaki sauce, and DI water plotted using Unistat. Figure 5 shows the rotated 3D view of the above results for higher visibility. The

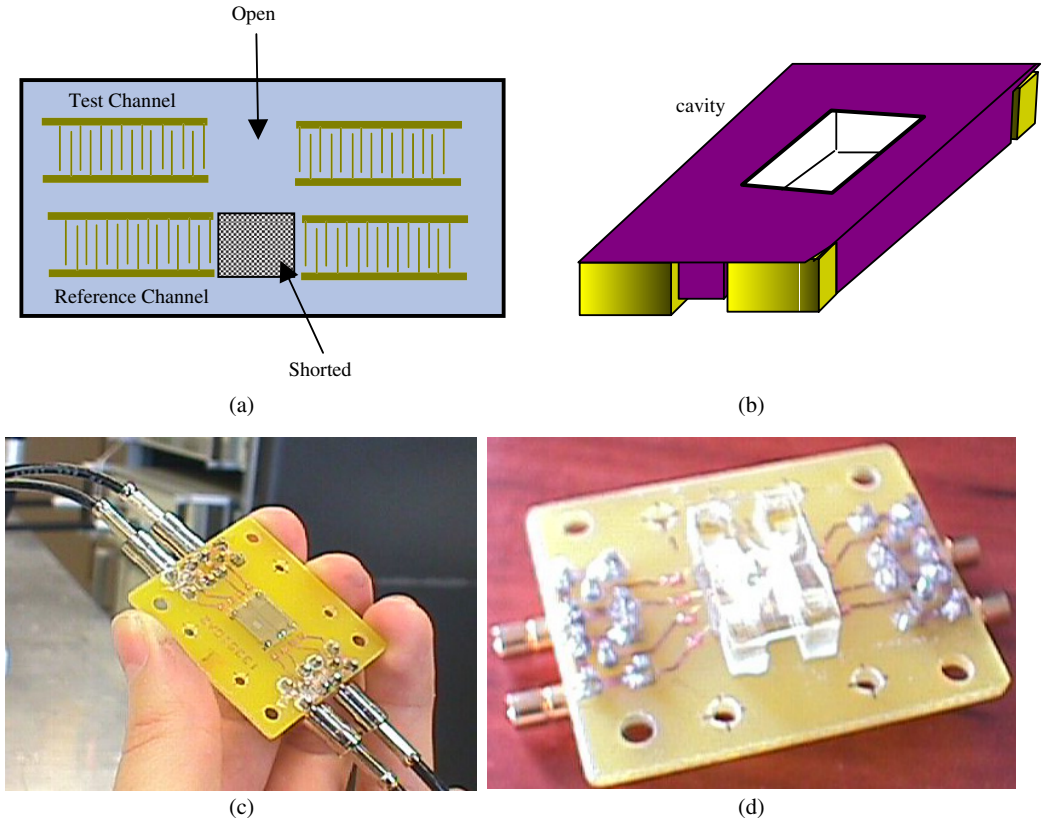

Figure 2. (a) Schematic diagram of (a) sensor; (b) microfluidic cell (dimensions are given in table 2); photograph of the fabricated device (c) without and (d) with microfluidic cell.

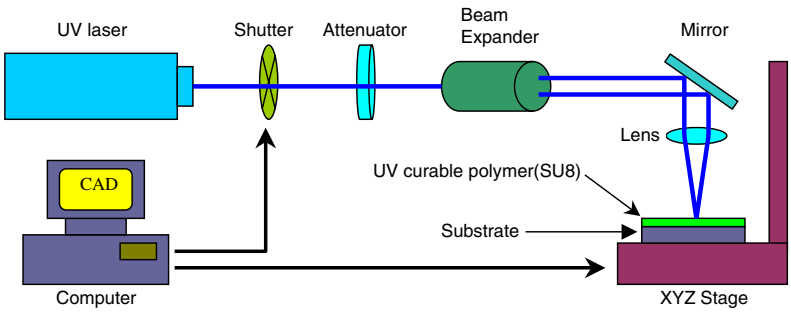

Figure 3. Schematic diagram of the MSL system for fabrication of the microfluidic cell.

difference between the amplitude and phase of the shorted and free surfaces is used for the data analysis in Minitab and the results are shown in figure 6. To study the effect of pH level of different liquids, scaling of pH values has been done on DI water. Hydrochloric acid was added to decrease the pH of the DI water, and sodium hydroxide was used to increase the pH. Figures 7 and 8 show the results of the measurements made on Strawberry Hi-C, teriyaki sauce and water.

The parameter reduction in the analysis is also attempted by taking the ratios and/or differences of free and shorted delay line phases and amplitudes. Figure 9 presents the PCA plot using Unistat on amplitude difference and phase difference ratios of free and shorted delay lines. It is clearly evident from these results that the identification of liquids is possible using the SAW microsensor.

6. Conclusions

Development of a compact microsensor along with a polymer microfluidic cell as part of an electronic tongue–nose combination is presented in this paper. The SH-SAW microsensors are fabricated on 36°-rotated Y-cut X-propagating $LiTaO_3$ ($36YX$.LT) substrate. This design consists of a dual-delay-line configuration in which one line is free and other one is metallized and shielded. Polymer microfluidic cells were designed and fabricated on top of it using a microstereolithography system to avoid dielectric loading of the IDTs by liquid which leads to unwanted dielectric sensitivity to the sensor. Testing of different liquids and soft drinks was done using an SAW microsensor. It can be seen from the test results that the measured results are

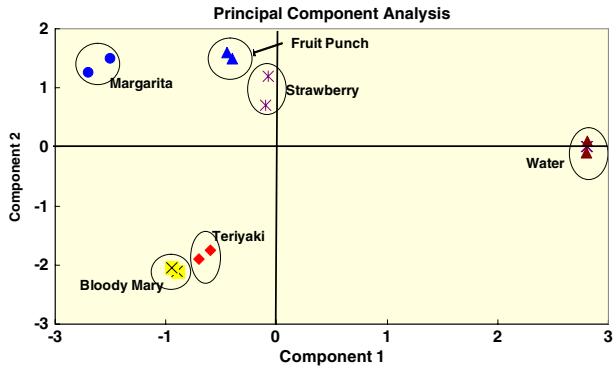

Figure 4. 2D view of the Unistat results: testing done on Strawberry Hi-C, Fruit Punch Hi-C, Margarita Mixer, DI water, Bloody Mary Mixer, and Teriyaki Sauce.

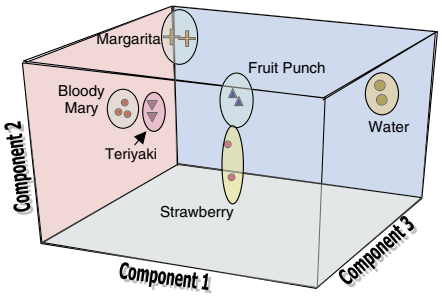

Figure 5. Rotated 3D view of testing done on Strawberry Hi-C, Fruit Punch Hi-C, Margarita Mixer, DI water, Bloody Mary Mixer, and teriyaki sauce.

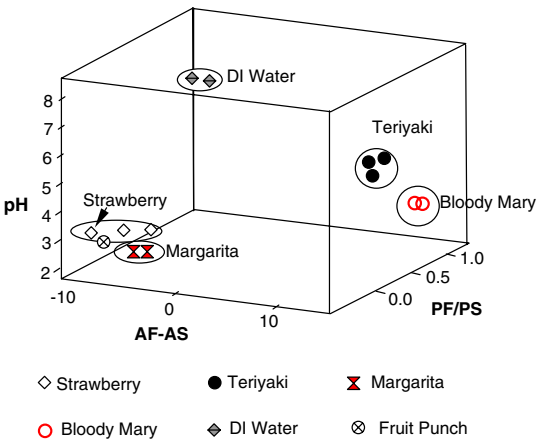

Figure 6. Plot generated using Minitab for the test done on Strawberry Hi-C, Fruit Punch Hi-C, Margarita Mixer, DI water, Bloody Mary Mixer, and teriyaki sauce.

consistent in classifying different liquids. In particular, it can be seen that Strawberry Hi-C, DI water, and teriyaki sauce separate out very nicely. Identification of liquids based on pH scale was a success as well. Attempts were also made for the identification of Fruit Punch Hi-C, Margarita Mixer, Bloody Mary Mixer, teriyaki sauce and DI water.

It can be seen from the data analysis that the SAW microsensor sensor is a very good device for use in the

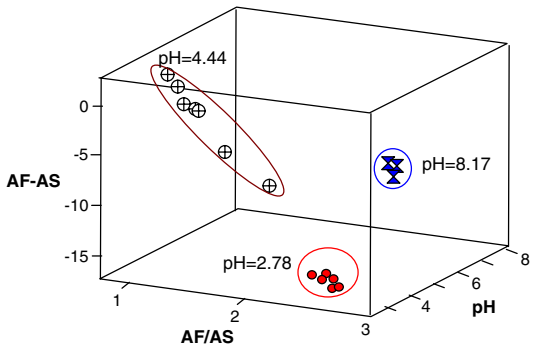

Figure 7. Plot generated for the test done on Strawberry Hi-C (2.78), teriyaki sauce (4.44) and pH scaled water (8.17).

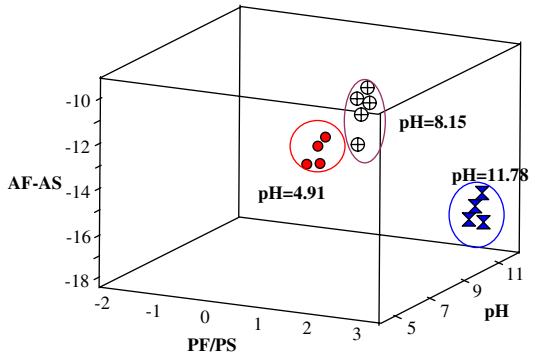

Figure 8. Plot of testing done on pH scaled liquids (HCl and sodium hydroxide additives).

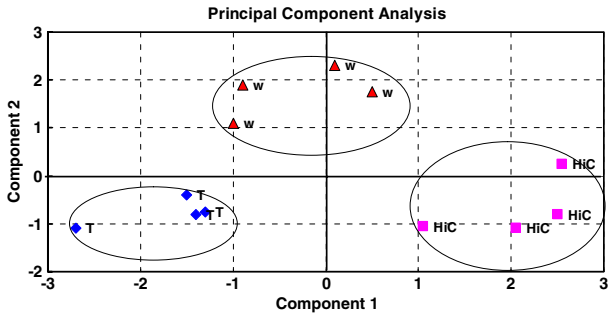

Figure 9. PCA plot using Unistat on amplitude difference and phase difference ratios between two delay lines: DI water (W), Hi-C strawberry fruit drink (HiC) and teriyaki sauce (T).

distinction of various liquids and liquid properties. It is obvious that this microsensor is able to use biological liquids for further testing. Because of the relatively low cost of the devices and the compatibility with CMOS fabrication, these microsensors have commercial applications in the food and beverage industries for disposable wireless sensors. They are ideal for inclusion on beverage packages for the purpose of distinguishing the age (freshness) of consumable liquids for quality control.

Not only can this SAW microsensor detect many unknown chemicals, but the strength (pH in many cases of liquids) can be detected as well. An electronic tongue–nose combination is proposed for targeting homeland security, wherein the tongue will evaluate the liquid while the nose will evaluate the head

space [24]. This combination will prove even more reliable and accurate in the classification of substances. One of the possible applications of these microsensors is water pollution detection in a stream or other water supply system. The data analysis presented in this paper can certainly be done in a more time and cost efficient manner using modern microprocessors and integrated circuits.

References

[1] Gardner J W and Bartlett P N 1999 *Electronic Noses: Principle and Applications* (Oxford: Oxford University Press)

[2] Ballantine D S, White R M, Martin S J, Ricco A J, Zellers E T, Frye G C and Wohltjen H 1997 *Acoustic Wave Sensors: Theory, Design and Physico-Chemical Applications* (New York: Academic)

[3] Kondoh J, Saito K, Shiokawa S and Suzuki H 1996 Simultaneous measurement of liquid properties using shear horizontal surface acoustic wave sensors *Japan. J. Appl. Phys.* 1 **35** 3093

[4] Dieulesaint E, Royer D, Legras O and Boubenider F 1987 A guided wave liquid level sensor *Proc. 1987 Ultrasonics Symp.* pp 569–72

[5] Moriizumi T, Unno Y and Shiokawa S 1987 New sensor in liquid using leaky SAW *Proc. 1987 Ultrasonics Symp.* pp 579–82

[6] Herrmann F, Hahn D and Buttgenbach S 1999 Separate determination of liquid density and viscosity with sagittally corrugated Love-mode sensors *Sensors Actuators* A**78** 99–107

[7] Nomura T, Uchiyama M, Saitoh A and Furukawa S 1998 Measurement of acoustic properties of liquids using SH and R-mode surface acoustic wave *Proc. 1998 Int. Freq. Control Symp.* pp 645–51

[8] Nomura T, Uchiyama M, Saitoh A and Furukawa S 1998 Surface acoustic wave liquid sensor using dual mode delay line *Proc. IEEE Symp. on Applications of Ferroelectrics* (Piscataway, NJ: IEEE) pp 289–92

[9] Yamazaki T, Kondoh J, Matsui Y and Shiokawa S 2000 Estimation of components and concentration in mixture solutions of electrolytes using a liquid flow system with SH-SAW sensor *Sensors Actuators* A **83** 34–9

[10] Kondoh J and Shiokawa S 1995 Liquid identification using SH-SAW sensors *Proc. Transducers-95* pp 716–9

[11] Campitelli A P, Wlodarski W and Hoummandy M 1998 Identification of natural spring water using shear horizontal SAW based sensors *Sensors Actuators* B **49** 195–201

[12] Kondoh J, Matsui Y and Shiokawa S 2003 Identification of electrolytic solutions using horizontal surface acoustic wave sensor with a liquid-flow system *Sensors Actuators* B **91** 309–15

[13] Nanto H, Tsubakino S, Ikeda M and Endo F 1995 Identification of aromas from wine using quartz-resonator gas sensors in conjunction with neural-network analysis *Sensors Actuators* B **24/25** 794–6

[14] Campbell C K 1998 *Surface Acoustic Wave Devices for Mobile and Wireless Communications* (New York: Academic) chapter 11

[15] Moriizumi T, Unno Y and Shikawa S 1987 New sensor in liquid using leaky SAW *Proc. 1987 IEEE Ultrasonic Symp. (Denver, CO)* (Piscataway, NJ: IEEE) pp 579–82

[16] Cole M, Sehra G, Gardner J W and Varadan V K 2004 Development of smart tongue devices for measurement of liquid properties *IEEE Sensors J.* **4** 543–50

[17] Kondoh J and Shiokawa S 1992 Liquid sensor based on shear horizontal SWA devices *Trans. IEICE, J75-C-II (May 1992)* pp 224–64 (in Japanese)
Kondoh J and Shiokawa S 1993 *Electron. Commun. Japan* 2 **76** 69–82 (Engl. Transl.)

[18] Kondoh J and Shiokawa S 1994 Shear surface acoustic wave liquid sensor based on acoustoelectric interaction *Trans. IEICE (J77-CII, 8, August)* pp 338–47 (in Japanese)
Kondoh J and Shiokawa S 1995 *Electron. Commun. Japan* 2 **78** 101–12 (Engl. Transl.)

[19] Barrow G M 1979 *Physical Chemistry* (New York: McGraw-Hill)

[20] Jacesko S L, Ji T, Abraham J K, Varadan V K and Gardner J W 2003 Design of a microfluidic cell using microstereolithogtaphy for electronic tongue applications *Proc. SPIE Smart Struct. Mater.* **5055** 147–53

[21] Curtin S D, Jakoby B, Berthold A, Varadan V K, Varadan V V and Vellekoop M J 1998 A micromachined wet cell for a Love-wave liquid sensor *Proc. SPIE Smart Electron. MEMS* **3328** 194–200

[22] Bertsch A, Lorenz H and Renaud P 1999 3D microfabrication by combining microstereolithography and thick resist UV lithography *Sensors Actuators* A **73** 14–23

[23] Varadan V K, Jiang X and Varadan V V 2002 *Microstereolithography* (New York: Wiley)

[24] Varadan V K and Gardner J W 1999 Smart tongue and nose *Proc. SPIE Smart Electron. MEMS* **3673** 67–75